

## Thermally Controlled Intracellular Uptake System of Polymeric Micelles Possessing Poly(*N*-isopropylacrylamide)-Based Outer Coronas

Jun Akimoto,<sup>†,‡</sup> Masamichi Nakayama,<sup>\*,†</sup> Kiyotaka Sakai,<sup>‡</sup> and Teruo Okano<sup>\*,†</sup>

*Institute of Advanced Biomedical Engineering and Science, Tokyo Women's Medical University (TWIns), Kawada-cho 8-1, Shinjuku-ku, Tokyo 162-8666, Japan, and Department of Applied Chemistry, Waseda University, Ohkubo 3-4-1, Shinjuku-ku, Tokyo 169-8555, Japan*

Received January 28, 2010; Revised Manuscript Received May 1, 2010; Accepted May 11, 2010

**Abstract:** Temperature-induced intracellular uptake mechanism of thermoresponsive polymeric micelles comprising poly(*N*-isopropylacrylamide-*co*-*N,N*-dimethylacrylamide)-*b*-poly(D,L-lactide) (P(IPAAm-DMAAm)-*b*-PLA) inside cultured bovine carotid endothelial cells is investigated by flow cytometry and confocal laser scanning microscopy. Hydrodynamic sizes of P(IPAAm-DMAAm)-*b*-PLA micelles are approximately 20 nm below the lower critical solution temperature (LCST) of 39.4 °C, and their sizes increased to *ca.* 600 nm above the LCST due to the aggregation of micelles. Intracellular uptake of P(IPAAm-DMAAm)-*b*-PLA micelles is significantly limited at a temperature below the micellar LCST, 37 °C. Of great interest, the P(IPAAm-DMAAm)-*b*-PLA micelles are internalized into the cells above the micellar LCST (42 °C), being dependent on polymer concentration, time, and temperature. By contrast, no intracellular uptake of polyethylene glycol-*b*-PLA micelles is observed regardless of temperature changes. Enhanced intracellular micelle uptake is probably due to the enhanced interactions between the micelles and cell membranes through the dehydration of corona-forming thermoresponsive polymer chains. Internalization of submicrometer-scale micellar aggregates inside the cells is probably due to their various endocytosis mechanisms. P(IPAAm-DMAAm)-*b*-PLA micelles localize at the Golgi apparatus and endoplasmic reticulum, but not inside lysosomes. These results indicate that the thermoresponsive polymeric micelles are greatly promising as intracellular delivery tools of drugs, nucleic acids, and peptides/protein without lysosomal decomposition in conjunction with applied heating.

**Keywords:** Polymeric micelle; thermoresponsive system; poly(*N*-isopropylacrylamide); block copolymer; intracellular uptake

### Introduction

Spherical core–corona architectures of amphiphilic block copolymers—polymeric micelles—demonstrate a reliable structural stability and a nanoscale size in aqueous media.

\* Corresponding authors: Institute of Advanced Biomedical Engineering and Science, Tokyo Women's Medical University (TWIns), Kawada-cho 8-1, Shinjuku-ku, Tokyo 162-8666, Japan. Tel: +81-3-5367-9945 (ext 6201). Fax: +81-3-3359-6046. E-mail: tokano@abmes.twmu.ac.jp; mnakayama@abmes.twmu.ac.jp.

<sup>†</sup> Tokyo Women's Medical University.

<sup>‡</sup> Waseda University.

Hydrophobic cores play a role of incorporating a large amount of various drugs, and densely packed hydrophilic polymer layers as micellar coronas can reduce interactions with serum proteins and tissues.<sup>1</sup> In addition, nanosized particles in a range of 10–200 nm can achieve long circulation in the bloodstream with avoiding the body's defense systems (reticuloendothelial system, RES), rapid kidney excretion,<sup>1</sup> and subsequent accumulation at tumor tissues due to tumor characteristic properties called the

(1) Kataoka, K.; Kwon, G. S.; Yokoyama, M.; Okano, T.; Sakurai, Y. Block copolymer micelles as vehicles for drug delivery. *J. Controlled Release* **1993**, 24 (1–3), 119–132.

enhanced permeability and retention (EPR) effect.<sup>2</sup> Because of these advantages as biocompatible materials, polymeric micelles have been extremely attractive for tumor-targeted drug carriers.<sup>1,3</sup> Recently, intracellular drug and gene delivery using polymeric carriers have been actively studied to achieve more effective and site-specific therapeutic systems. For instance, a large amount of drugs with carrier-loading state inside cells can overcome efflux pump activity of multidrug-resistant cells.<sup>4</sup> Moreover, the intracellular delivery of nucleic acid related compounds using polymeric vectors results in an efficient gene therapy. Efficiency of carrier internalization is known to depend on the physicochemical properties of polymeric carriers. Cellular membranes charge negatively because of negatively charged molecules such as sialic acids found on the membranes and hold numerous glycoproteins on their heterogeneous surfaces, and thus cationic or hydrophobic molecules tend to internalize into cells by enhancing interactions with cellular membranes.<sup>5–7</sup> In contrast, for *in vivo* delivery uses, nanoparticles are required to circulate in blood stably avoiding interactions with proteins, nontargeting cells, and nontargeting tissues.

To resolve these contradictory conditions, stimuli-responsive carrier systems which change their features and/or structures in response to physicochemical signals including heat, local pH, and ultrasound are attractive strategies.<sup>8</sup> Among these possible signals, raised temperature is one of the most preferable due to easy-to-use approach, relative noninvasiveness, and a wide range of medical applications such as hyperthermia therapy.<sup>9</sup>

Poly(*N*-isopropylacrylamide) (PIPAAm) is a widely applied thermoresponsive polymer, which demonstrates a

reversible hydrophilic/hydrophobic property change through the phase transition at its lower critical solution temperature (LCST) of 32 °C in aqueous media.<sup>10</sup> In addition, PIPAAm's LCST can be easily modulated for desirable temperatures to utilize their biomedical applications by the introduction of hydrophilic or hydrophobic comonomers into the PIPAAm main chains. By using these unique features, many types of intelligent systems were proposed in biomaterial and drug delivery fields.<sup>11</sup> Our groups have developed polymeric micelle possessing thermoresponsive PIPAAm-based coronas as an intelligent drug targeting carrier system.<sup>12,13</sup> Corona-forming thermoresponsive polymers reversibly alter their conformation and water solubility through dehydration of the polymer chains across their LCST. Temperature-induced property changes of the polymeric micelles demonstrate the acceleration of incorporated drug release rates and subsequent *in vitro* cytotoxicity for various cultured cells.<sup>14–17</sup> Our strategy using thermoresponsive micelle carriers for *in vivo* cancer chemotherapy is as follows. After accumulation of drug-loaded carriers at solid tumor tissues through the EPR-mediated delivery, site-specific drug action can be regulated by tumor-selective local heating with microwave-based hyperthermia and focused ultrasound.<sup>9</sup> Recently, our group successfully reported that the intracellular uptake of thermoresponsive micelles comprising P(IPAAm-*co*-*N,N*-dimethylacrylamide)-*b*-P(D,L-lactide) (P(IPAAm-DMAAm)-*b*-PLA) can be promoted by simply heating above the micellar LCST<sup>18</sup> (Figure 1). Although the temperature-dependent intracellular micelle uptake system is probably caused by

- (2) Matsumura, Y.; Maeda, H. A new concept for macromolecular therapeutics in cancer chemotherapy: mechanism of tumoritropic accumulation of proteins and the antitumor agent smancs. *Cancer Res.* **1986**, *46* (12), 6387–6392.
- (3) Torchilin, V. P. Micellar nanocarriers: pharmaceutical perspectives. *Pharm. Res.* **2007**, *24* (1), 1–16.
- (4) Lee, E. S.; Na, K.; Bae, Y. H. Doxorubicin loaded pH-sensitive polymeric micelles for reversal of resistant MCF-7 tumor. *J. Controlled Release* **2005**, *103* (2), 405–418.
- (5) Merdan, T.; Kopecek, J.; Kissel, T. Prospects for cationic polymers in gene and oligonucleotide therapy against cancer. *Adv. Drug Delivery Rev.* **2002**, *54* (5), 715–758.
- (6) Gratton, S. E. A.; Ropp, P. A.; Pohlhaus, P. D.; Luft, J. C.; Madden, V. J.; Napier, M. E.; DeSimone, J. M. The effect of particle design on cellular internalization pathways. *Proc. Natl. Acad. Sci. U.S.A.* **2008**, *105* (33), 11613–11618.
- (7) Miller, C. R.; Bondurant, B.; McLean, S. D.; McGovern, K. A.; O'Brien, D. F. Liposome-cell interactions *in vitro*: effect of liposome surface charge on the binding and endocytosis of conventional and sterically stabilized liposomes. *Biochemistry* **1998**, *37* (37), 12875–12883.
- (8) Ganta, S.; Devalapally, H.; Shahiwal, A.; Amiji, M. A review of stimuli-responsive nanocarriers for drug and gene delivery. *J. Controlled Release* **2008**, *126* (3), 187–204.
- (9) Kong, G.; Anyambhatla, G.; Petros, W. P.; Braun, R. D.; Colvin, O. M.; Needham, D.; Dewhirst, M. W. Efficacy of liposomes and hyperthermia in a human tumor xenograft model: importance of triggered drug release. *Cancer Res.* **2000**, *60* (24), 6950–6957.
- (10) Heskins, M.; Guillet, J. E. Solution properties of poly(*N*-isopropylacrylamide). *J. Macromol. Sci., Chem.* **1968**, *2* (8), 1441–1455.
- (11) Okano, T.; Bae, Y. H.; Kim, S. W. Temperature responsive controlled drug delivery. In *Pulsed and Self-Regulated Drug Delivery*; Kost, J., Ed.; CRC Press: Boca Raton, FL, 1990; 17–46.
- (12) Cammas, S.; Suzuki, K.; Sone, C.; Sakurai, Y.; Kataoka, K.; Okano, T. Thermo-responsive polymer nanoparticles with a core-shell micelle structure as site-specific drug carriers. *J. Controlled Release* **1997**, *48* (2–3), 157–164.
- (13) Nakayama, M.; Okano, T. Intelligent thermoresponsive polymeric micelles for targeted drug delivery. *J. Drug Delivery Sci. Technol.* **2006**, *16* (1), 35–44.
- (14) Chung, J. E.; Yokoyama, M.; Okano, T. Inner core segment design for drug delivery control of thermo-responsive polymeric micelles. *J. Controlled Release* **2000**, *65* (1–2), 93–103.
- (15) Kohori, F.; Sakai, K.; Aoyagi, T.; Yokoyama, M.; Yamato, M.; Sakurai, Y.; Okano, T. Control of adriamycin cytotoxic activity using thermally responsive polymeric micelles composed of poly(*N*-isopropylacrylamide-*co*-*N,N*-dimethylacrylamide)-*b*-poly-(D,L-lactide). *Colloids Surf., B* **1999**, *16* (1–4), 195–205.
- (16) Nakayama, M.; Okano, T.; Miyazaki, T.; Kohori, F.; Sakai, K.; Yokoyama, M. Molecular design of biodegradable polymeric micelles for temperature-responsive drug release. *J. Controlled Release* **2006**, *115* (1), 46–56.
- (17) Soppimath, K. S.; Liu, L. H.; Seow, W. Y.; Liu, S. Q.; Powell, R.; Chan, P.; Yang, Y. Y. Multifunctional core/shell nanoparticles self-assembled from pH-induced thermosensitive polymers for targeted intracellular anticancer drug delivery. *Adv. Funct. Mater.* **2007**, *17* (3), 355–362.

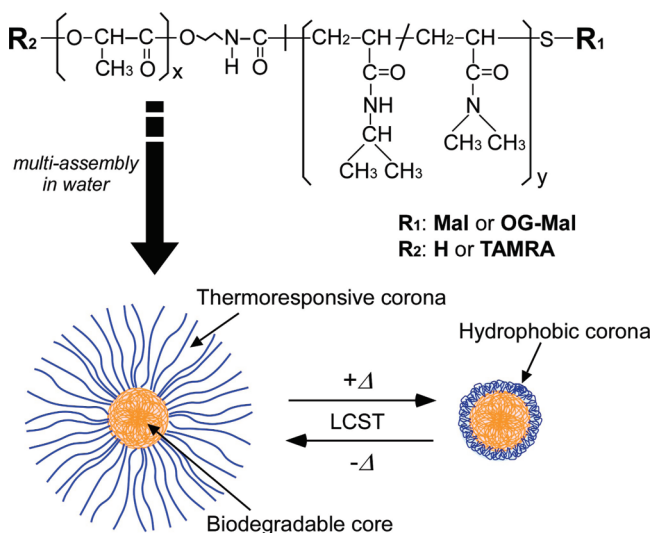


**Figure 1.** Chemical structure of thermoresponsive block copolymers of P(IPAAm-DMAAm)-*b*-PLA and temperature-induced property change of polymeric micelle possessing thermoresponsive corona across its LCST.

the enhancement of interactions between cells and the micelles mediated through the thermoresponsive phase transition of the micellar coronas, the intracellular micelle uptake mechanism and the micelle distributions are unclear. This study investigated the temperature-dependent uptake mechanism and intracellular micelle distributions of the micelles by confocal laser scanning microscopy and flow cytometry.

## Experimental Section

**Materials.** IPAAm was kindly provided by Kojin (Tokyo, Japan) and purified by recrystallization from *n*-hexane. DMAAm (Wako Pure Chemicals, Osaka) was distilled under reduced pressure. *N,N*-Dimethylformamide (DMF), 2,2'-azobis[2-methyl-*N*-(hydroxyethyl)]propionamide (VA-086), 1,4-dioxane, tetrahydrofuran, *N,N*-dimethylacetamide, xylene, and diethyl ether were purchased from Wako Pure Chemicals and were used without further purification. D,L-Lactide (LA) (Tokyo Chemical Industry, Tokyo) was recrystallized from ethyl acetate. Maleimide (Mal) (Aldrich, St. Louis, MO), 2-hydroxyethylamine (Kanto Chemical, Tokyo), tin(II) 2-ethylhexanoate (Aldrich), PEG methyl ether (the number-averaged molecular weight: approximately 5000) (Aldrich), Oregon Green 488 maleimide (Invitrogen, Carlsbad, CA), and tetramethylrhodamine-5-carbonyl azide (TAMRA) (Invitrogen) were used as received. A reversible addition-fragmentation chain transfer agent, 2-[*N*-(2-hydroxyethyl)carbamoyl]prop-2-yl dithiobenzoate, was prepared according to a previously published procedure.<sup>19</sup> Water used in this study was purified by a Milli-Q Synthesis A10 system (Millipore, Billerica, MA) unless otherwise mentioned.

**Preparation of Diblock Copolymers.**  $\alpha$ -Hydroxyl,  $\omega$ -thiobenzoylthio-P(IPAAm-DMAAm) was synthesized by RAFT polymerization using a RAFT agent, 2-cyanopropyl dithiobenzoate as in our previous report.<sup>18</sup> Thiobenzoylthio-terminated P(IPAAm-DMAAm)-*b*-PLA was prepared by ring-opening polymerization of LA initiated from terminal hydroxyl group of P(IPAAm-DMAAm).<sup>18</sup> PEG-*b*-PLA was synthesized by a procedure similar to that used for the synthesis of thermoresponsive block copolymers. Briefly, PEG ( $1.0 \times 10^{-4}$  mol) and LA ( $2.0 \times 10^{-3}$  mol) were dried under reduced pressure for 2 h. Tin(II) 2-ethylhexanoate (15 mg) as a catalyst and deoxidized xylene (10 mL) were added, and polymerization was carried out at 140 °C for 20 h in a nitrogen atmosphere. After the polymerization, polymers were recovered by the repeated precipitation with an excess amount of diethyl ether and then dried *in vacuo*. The obtained polymers were characterized by <sup>1</sup>H NMR (400 MHz) (Varian, Palo Alto, CA) and gel permeation chromatography (GPC). GPC analysis was performed by a GPC system (SC-8020) (Tosoh, Tokyo) with two columns (TSKgel-G3000H HR and TSKgel-G4000H HR) (Tosoh) at 45 °C using DMF containing LiCl (50 mmol/L) as an eluent (the flow rate: 1.0 mL/min) and calibrated with polyethylene oxide standards.

**Conversion of Polymer Termini Functional Groups.** Fluorescent molecules were introduced to the block copolymer termini. The conjugation of the thermoresponsive segment termini with maleimide derivatives was described in our previous report.<sup>18</sup> TAMRA labeling on PLA termini was performed according to Luo's methods.<sup>20</sup> Block copolymers and TAMRA (5 mol equivalents versus polymer termini) were dissolved in deoxidized DMF (3 mL), and then reactions were carried out at 80 °C for 5 h in a nitrogen atmosphere under a dark condition. After the reaction, polymer solution was dialyzed against methanol using a dialysis membrane (Spectra/Por 6, MWCO 1000) (Spectrum Laboratories, Rancho Dominguez, CA) for 4 days, and subsequently dialyzed against water until complete removal of unreacted TAMRA and byproducts. Polymers were recovered by lyophilization as powder. The efficiency of TAMRA introduction was confirmed by using an FP-6500 spectrofluorimeter (JASCO, Tokyo). Excitation and emission bandwidths were 5 and 3 nm, respectively. The intensity of fluorescence ( $E_x$ , 545 nm;  $E_m$ , 570 nm) was measured in dimethyl sulfoxide.

**Preparation and Characterization of Polymeric Micelles.** Formation of polymeric micelles was simultaneously performed by an aqueous dialysis method.<sup>15</sup> General preparation of fluorescent labeled polymeric micelles was as

(18) Akimoto, J.; Nakayama, M.; Sakai, K.; Okano, T. Temperature-induced intracellular uptake of thermoresponsive polymeric micelles. *Biomacromolecules* **2009**, *10* (6), 1331–1336.

(19) Chong, Y. K.; Krstina, J.; Le, T. P. T.; Moad, G.; Postma, A.; Rizzardo, E.; Thang, S. H. Thiocarbonylthio compounds [ $\text{S}=\text{C}(\text{Ph})\text{S}-\text{R}$ ] in free radical polymerization with reversible addition-fragmentation chain transfer (RAFT polymerization). role of the free-radical leaving group (R). *Macromolecules* **2003**, *36* (7), 2256–2272.

(20) Luo, L.; Tam, J.; Maysinger, D.; Eisenberg, A. Cellular internalization of poly(ethylene oxide)-*b*-poly( $\epsilon$ -caprolactone) diblock copolymer micelles. *Bioconjugate Chem.* **2002**, *13* (6), 1259–1265.

follows: A polymer mixture of Mal- and OG-P(IPAAm-DMAAm)-*b*-PLA (Mal/OG = 80/20 (w/w %)) in polymer was dissolved in *N,N*-dimethylacetamide, and then the solutions were dialyzed against water using a dialysis membrane (Spectra/Por 6, MWCO 1000) at 10 °C for 24 h under a dark condition.

Hydrodynamic micellar diameters and their distributions in Dulbecco's phosphate buffered saline without calcium chloride and magnesium chloride (DPBS(−), pH 7.4) (Sigma) were determined by dynamic light scattering using a Nano-ZS instrument (Malvern Instruments, Worcestershire, U.K.) equipped with a He–Ne laser (633 nm) at a scattering angle of 173°.

Optical transmittance of the polymeric micelles (5.0 mg/mL) in DPBS(−) at various temperatures was measured at 600 nm by a UV–vis spectrophotometer (V-530) (JASCO) with a sample cell thermostat (EHC-477S) (JASCO). The heating rate was 0.1 °C/min. The LCSTs of the micelle solutions were defined as the temperature producing a 50% decrease in optical transmittance.

**Cell Culture.** Bovine carotid endothelial cells (EC) (Health Science Research Resources Bank, Osaka) were cultured in Dulbecco's modified Eagle's medium (DMEM) (Sigma) supplemented with 10% fetal bovine serum (FBS) (Bioserum, Victoria, Australia), penicillin (50 unit/mL), and streptomycin (50 µg/mL) at 37 °C under 5% CO<sub>2</sub> condition. Cells were cultured for 2 days to achieve almost confluent conditions before performing all experiments.

**Confocal Laser Scanning Microscopy (CLSM).** ECs were seeded into 4-well Lab-Tek chambered cover glasses (2.0 × 10<sup>5</sup> cells/mL, 500 µL/well) (Nalge Nunc International, Rochester, NY), and then cultured for 2 days. Cultured cells were incubated in DMEM/FBS including OG-labeled micelles (200 µg/mL) at temperatures below (37 °C) or above (42 °C) the LCST in a humidified atmosphere with 5% CO<sub>2</sub>. After incubation, ECs were rinsed with DMEM/FBS three times and incubated for another 10 min with LysoTracker Red (200 nmol/L in DMEM) (Invitrogen) or Brefeldin A BODIPY 558/568 conjugate (100 nmol/L in DMEM) (Invitrogen) at 37 °C. Cell nuclei were stained with Hoechst 33258 (Invitrogen) for 5 min, followed by two rinses with DPBS(−). Samples were visualized by a confocal laser scanning microscopy, ConfoCor3 LSM510 META (Carl Zeiss, Oberkochen, Germany) with diode (405 nm), Ar (488 nm), and diode-pumped solid state (DPSS, 561 nm) lasers at room temperature.

**Flow Cytometry.** ECs were seeded into 4-well multidishes (2.0 × 10<sup>5</sup> cells/mL, 500 µL/well) (Nalge Nunc International), followed by 2-day culture. ECs were incubated with polymer micelles (50–400 µg/mL) in DMEM/FBS at various temperatures (37–45 °C) across the micellar LCST (40 °C). Furthermore, incubation temperature was repeatedly changed across the micellar LCST (37 and 42 °C) to investigate the effects of temperature changes on the intracellular micelle uptake. After incubation for various periods, ECs were gently rinsed with DMEM/FBS to remove non-intracellular OG-labeled micelles, followed by treatment with 0.05% trypsin–

ethylenediaminetetraacetic acid (Sigma). Recovered cells were rinsed with DPBS(−) twice, and propidium iodide (1 µL, 1 mg/mL) (Invitrogen) was added to the sample solutions. Cellular uptake was estimated using an EPICS XL-MCL flow cytometer (Beckman Coulter, Fullerton, CA) at room temperature, and 10000 events were analyzed using EXPO2 software.

**Analysis of Endocytosis Pathways.** ECs were seeded into 24-well multidishes (2.0 × 10<sup>5</sup> cells/mL, 500 µL/well) (BD Falcon, Franklin Lakes, NJ), followed by 2-day culture. Prior to incubation with the polymer micelles, endocytosis inhibiting reagents were incubated for 60 min at 37 °C in DMEM supplemented with filipin (10 µg/mL) (Sigma), genistein (400 mmol/L) (Sigma), chlorpromazine (30 µmol/L) (Sigma), sucrose (900 mmol/L) (Wako pure chemical), amiloride (2 mmol/L) (Sigma) or cytochalasin B (250 µmol/L) (Sigma). After preincubation, cells were gently rinsed with DMEM/FBS three times. ECs were incubated with the polymer micelles (200 µg/mL) in DMEM/FBS at 42 °C for 3 h. After incubation, ECs were recovered and analyzed by the flow cytometer by the same protocols as mentioned above.

## Results and Discussion

**Preparation and Characterization of Block Copolymers.** RAFT polymerization involves a conventional free radical polymerization of various monomers in the presence of dithiobenzoate compound as a chain transfer agent, and allows for control of polymer molecular weight and its distribution during the polymerization process.<sup>21,22</sup>  $\alpha$ -Hydroxyl,  $\omega$ -thiobenzoylthio-P(IPAAm-DMAAm) was synthesized by RAFT polymerization ( $M_n = 9300$ ,  $M_w/M_n = 1.08$ , monomer unit: IPAAm/DMAAm = 54/29).<sup>18</sup> Thiobenzoylthio-terminated P(IPAAm-DMAAm)-*b*-PLA was characterized by GPC and <sup>1</sup>H NMR ( $M_n = 11300$ ,  $M_w/M_n = 1.07$ , monomer unit: IPAAm/DMAAm/LA = 54/29/14).<sup>18</sup> Terminal conjugation of P(IPAAm-DMAAm)-*b*-PLA with maleimide (Mal) and its Oregon Green 488 (OG) derivative was performed according to a previously reported procedure.<sup>18</sup> Hydrophilic comonomer, *N,N*-dimethylacrylamide (DMAAm), was introduced to thermoresponsive IPAAm main chains to regulate the micellar LCST (*ca.* 40 °C) (higher than physiological temperature to utilize them in conjunction with medical heating system for hyperthermia treatment). Methoxy-polyethylene glycol-*b*-PLA (PEG-*b*-PLA) was synthesized by anionic ring-opening polymerization using tin(II) 2-ethylhexanoate as a catalyst. Chemical composition of PEG-*b*-PLA was estimated from the <sup>1</sup>H NMR proton signals

- (21) Chiefari, J.; Chong, Y. K. B.; Ercole, F.; Krstina, J.; Jeffery, J.; Le, T. P. T.; Mayadunne, R. T. A.; Meijs, G. F.; Moad, C. L.; Moad, G. Living free-radical polymerization by reversible addition-fragmentation chain transfer: The RAFT process. *Macromolecules* **1998**, *31* (16), 5559–5562.
- (22) Lowe, A. B.; McCormick, C. L. Reversible addition fragmentation chain transfer (RAFT) radical polymerization and the synthesis of water-soluble (co) polymers under homogeneous conditions in organic and aqueous media. *Prog. Polym. Sci.* **2007**, *32* (3), 283–351.

in CDCl<sub>3</sub> from EG methylene (3.6 ppm) and LA methine (5.1 ppm) protons (PEG/PLA: 114/18 (number of molecule)). Tetramethylrhodamine (TAMRA) was conjugated with the terminal hydroxyl groups of PLA segments according to a previous report.<sup>20</sup> Terminal conversion was estimated by fluorescent intensity ( $E_x$ , 545 nm;  $E_m$ , 570 nm) in dimethyl sulfoxide, and the conversion efficiencies of P(IPAAm-DMAAm)-*b*-PLA and PEG-*b*-PLA were 67.6 and 73.5%, respectively (coded as P(IPAAm-DMAAm)-*b*-PLA-TAMRA and PEG-*b*-PLA-TAMRA). Polydispersity index (PDI) of the block copolymers was determined by gel permeation chromatography (GPC). All obtained polymers demonstrated unimodal GPC curves with narrow PDI less than 1.15.

**Characterization of Polymeric Micelles.** Polymeric micelles were prepared by the dialysis of block copolymers in *N,N*-dimethylacetamide against water at 10 °C.<sup>15</sup> Closely packed hydrophobic or fluorescent moieties on the micellar surface possibly led to the micellar LCST shifts and fluorescent OG quenching. Therefore, fluorescent OG-labeled micelles comprising a mixture of OG- and Mal-P(IPAAm-DMAAm)-*b*-PLA copolymers at the ratio of 80/20 (w/w %) in the polymer were formed.<sup>23</sup> OG-labeled thermoresponsive micelles demonstrated their LCST at 39.4 °C and approximately 20 nm in diameter at 37 °C in Dulbecco's phosphate buffered saline without calcium chloride and magnesium chloride (DPBS(−)) solution. Increasing the temperature above the LCST to 42 °C, the micelles formed submicrometer-ordered aggregates (614 nm in diameter) due to enhanced intermicellar hydrophobic interactions through the dehydration of corona-forming thermoresponsive P(IPAAm-DMAAm) chains. In order to investigate the effects of the micellar thermoresponse on intracellular uptake, TAMRA-labeled polymeric micelles possessing thermoresponsive P(IPAAm-DMAAm) coronas or PEG-coronas were prepared from a polymer blend of TAMRA-conjugated block copolymers and nonconjugated block copolymers at various polymer weight ratios (for thermoresponsive micelles, Mal-P(IPAAm-DMAAm)-*b*-PLA/P(IPAAm-DMAAm)-*b*-PLA-TAMRA, 80/20; and for nonthermoresponsive micelles, PEG-*b*-PLA/PEG-*b*-PLA-TAMRA, 86/14) for avoiding fluorescent quenching at high concentration TAMRA units in the micellar cores.<sup>24</sup> Influence of introduced TAMRA moieties on the micellar properties was investigated by turbidity method, dynamic light scattering, and fluorescent measurements. The LCST value and the size of polymeric micelles possessing TAMRA units in the cores were found to be at the same level as those of nonlabeled micelles at both 37 and 42 °C in DPBS(−) solution. PEG-*b*-PLA micelles with TAMRA units in the cores showed approximately 40 nm in diameter by dynamic light scattering

**Table 1.** Characterization of Polymeric Micelles

block copolymers	diameter (nm)		LCST (°C) <sup>a</sup>
	37 °C	42 °C	
Mal-P(IPAAm-DMAAm)- <i>b</i> -PLA	23.3 ± 12.8	614 ± 274	40.0
OG-P(IPAAm-DMAAm)- <i>b</i> -PLA <sup>b</sup>	20.7 ± 8.5	589 ± 73.0	39.2
P(IPAAm-DMAAm)- <i>b</i> -PLA-TAMRA <sup>c</sup>	18.3 ± 7.3	579 ± 116	39.5
PEG- <i>b</i> -PLA	38.8 ± 16.7	38.9 ± 16.9	
PEG- <i>b</i> -PLA-TAMRA <sup>d</sup>	41.7 ± 17.3	41.6 ± 16.7	

<sup>a</sup> Determined by transmittance changes in DPBS(−) solution. Heating rate: 0.1 °C/min. <sup>b</sup> Mal-P(IPAAm-DMAAm)-*b*-PLA/OG-P(IPAAm-DMAAm)-*b*-PLA: 80/20 (w/w %). <sup>c</sup> (Mal-P(IPAAm-DMAAm)-*b*-PLA)/(Mal-P(IPAAm-DMAAm)-*b*-PLA-TAMRA): 70/30 (w/w %). <sup>d</sup> (PEG-*b*-PLA)/(PEG-*b*-PLA-TAMRA): 86/14 (wt%).

regardless of temperature changes. These results indicated that the introduction of TAMRA molecules scarcely affected the micellar properties. Fluorescent spectra of TAMRA-labeled P(IPAAm-DMAAm)-*b*-PLA and PEG-*b*-PLA micelles were measured by excitation wavelength at 545 nm and were clearly observed in the DPBS(−) solution. Characterization of these obtained polymeric micelles is summarized in Table 1.

#### Temperature-Induced Intracellular Uptake of Micelles.

Temperature effects on the cellular uptake of polymeric micelles into bovine carotid endothelial cells (ECs) were investigated by flow cytometry using OG-labeled P(IPAAm-DMAAm)-*b*-PLA micelles. A previous study reported that the outermost surface OG moiety was unable to affect the intracellular uptake and the cytotoxicity of micelles.<sup>18</sup> The relationship between the concentration and the intracellular uptake of micelles was investigated (Figure 2). The experiment was performed at various micellar concentrations (50–400 µg/mL), which was higher than their critical micelle concentration (23 µg/mL)<sup>18</sup> without polymer precipitation at 42 °C. The flow cytometric studies showed that fluorescent intensity derived from the incorporated micelles increased with increasing in the micellar concentration. In addition, the intracellular uptake of micelles was significantly promoted at an incubation temperature of 42 °C (above the LCST) compared with that of 37 °C (below the LCST).

Incubation temperature effect on the cellular uptake was investigated in a range of 37–45 °C (Figure 3). Cells on the culture plates were incubated with DMEM/FBS including 200 µg/mL of OG-labeled P(IPAAm-DMAAm)-*b*-PLA micelles for 6 h at each temperature. At temperatures below the micellar LCST (39.4 °C), the intracellular uptake of micelles was observed to be also negligible. Upon heating above the LCST, the fluorescent intensity was increased with increasing the temperatures. Interestingly, the efficiency of intracellular uptake steeply decreased over 43 °C and reached to the similar level as those below the LCST. Cellular viability was also estimated using propidium iodide for investigating relation between the intracellular uptake efficiency and the cellular viability at various temperatures. Cellular viabilities remained approximately 95% against the nontreated control cells with the micelles in a temperature

(23) Nakayama, M.; Okano, T. Polymer terminal group effects on properties of thermoresponsive polymeric micelles with controlled outer-shell chain lengths. *Biomacromolecules* **2005**, *6* (4), 2320–2327.

(24) Savic, R.; Luo, L.; Eisenberg, A.; Maysinger, D. Micellar nanocontainers distribute to defined cytoplasmic organelles. *Science* **2003**, *300* (5619), 615–618.

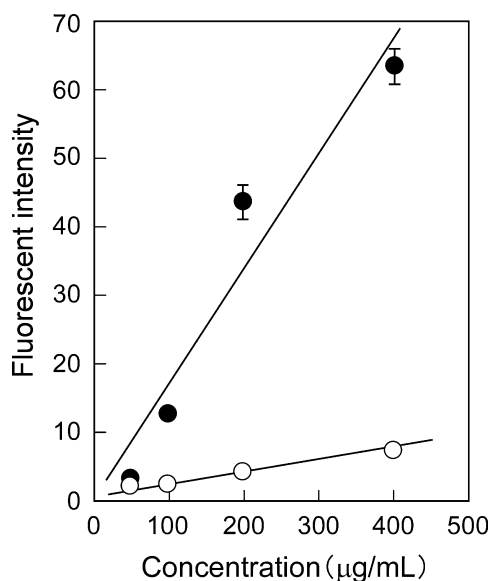


**Figure 2.** Relationship between the concentration and the intracellular uptake of P(IPAAm-DMAAm)-*b*-PLA micelles at temperatures below (37 °C) (open circles) and above (42 °C) (closed circles) micellar LCST. The circles and the bars show mean and standard deviation (SD), respectively ( $n = 4$ ). Incubation time: 6 h. Y axis: the mean fluorescent intensity of 10000 events.

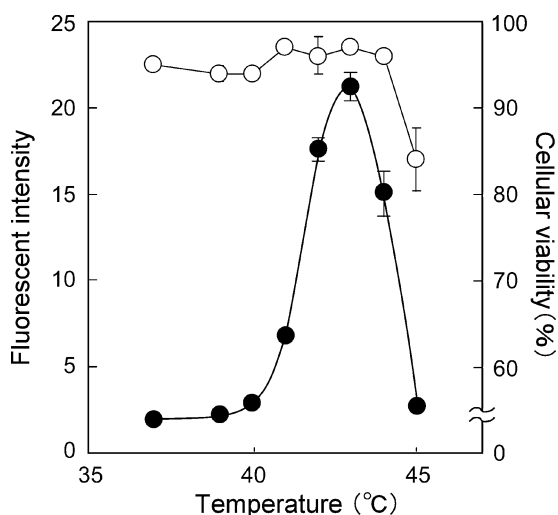


**Figure 3.** Temperature effects on the intracellular uptake of the P(IPAAm-DMAAm)-*b*-PLA micelles (closed circles) and cellular viability (open circles). Cellular viability was measured using propidium iodide. The circles and the bars show mean and SD, respectively ( $n = 4$ ). Incubation time: 6 h. Micelle concentration: 200  $\mu\text{g/mL}$  in DMEM/FBS. Y axis: the mean fluorescent intensity of 10000 events.

range of 37–44 °C, a slight decrease in viability was probably due to tryptic treatment to recover cells for the flow cytometric analysis. On the contrary, a significant decrease in cell viability was observed around 45 °C. This reduced cellular viability was possibly caused by the critical destruction of cellular functions through the denaturation of cellular proteins under extremely higher than physiological temper-

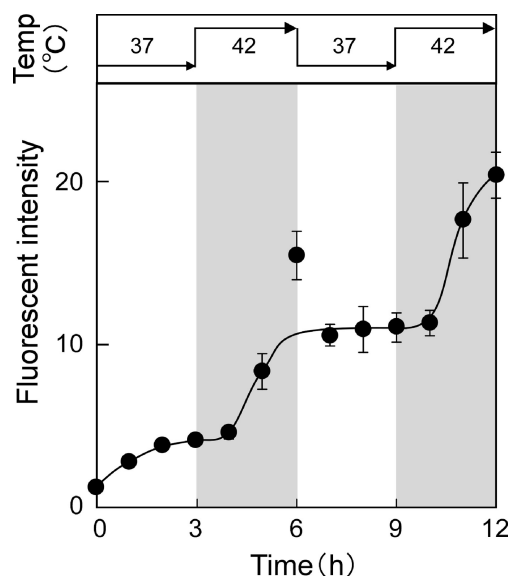


**Figure 4.** Intracellular uptake of P(IPAAm-DMAAm)-*b*-PLA micelles with temperature cycles between 37 and 42 °C. The circles and the bars show mean and SD, respectively ( $n = 4$ ). Micelle concentration: 200  $\mu\text{g/mL}$  in DMEM/FBS. Y axis: the mean fluorescent intensity of 10000 events.

ature,<sup>25</sup> resulting in a subsequent significant decrease in micelle uptake ability. The effects of repeated cycles across the LCST (37 and 42 °C) for 12 h on the intracellular uptake of P(IPAAm-DMAAm)-*b*-PLA micelles were also investigated (Figure 4). Although the intracellular uptake of the micelles was observed to be negligible below the LCST, the intracellular micelle uptake was significantly promoted by heating above the LCST. After cooling down the temperature below the LCST to 37 °C, the micellar internalization was limited again due to the reversibility of thermoresponse of P(IPAAm-DMAAm) chains. Consequently, the ON/OFF control of intracellular micelle uptake was successfully achieved by the repeatedly temperature cycles across the LCST.

To investigate the influence of corona-forming polymer thermoresponse on intracellular micelle uptake, differences in the intracellular uptake between thermoresponsive and non-thermoresponsive PEG-micelles, which were fluorescently labeled with TAMRA units in the cores, were estimated (Table 2). PEG-micelle uptake was at the same level of low efficiency as P(IPAAm-DMAAm)-*b*-PLA micelles at 37 °C. Intracellular uptake of PEG-micelles was unaffected by temperature change from 37 to 42 °C. This was speculated to be due to limiting of interactions with cellular membranes by the densely packed PEG chains on the micellar surface. We have previously reported that PEG block copolymers form core-shell micelle structure and densely packed PEG chains on micellar surface show a drastic decrease of interactions with serum proteins.<sup>1</sup> By

(25) Roti, R. J. L. Heat-induced cell death and radiosensitization: molecular mechanisms. *Natl. Cancer Inst. Monogr.* **1982**, 61, 3–10.

**Table 2.** Temperature-Dependent Intracellular Uptake of Polymeric Micelles Possessing PEG and Thermoresponsive Coronas<sup>a</sup>

micelle	37 °C	42 °C
PEG- <i>b</i> -PLA micelle	2.98 ± 0.30	3.48 ± 0.35
P(IPAAm-DMAAm)- <i>b</i> -PLA micelle	3.05 ± 0.30	10.1 ± 0.40

<sup>a</sup> Mean fluorescent intensity of 10000 events determined by flow cytometry. Incubation time: 24 h, micelle concentration: 200 µg/mL in DMEM/FBS.

contrast, the intracellular uptake of TAMRA-labeled thermoresponsive micelles was promoted over the micellar LCST of corona-forming P(IPAAm-DMAAm) chains similar to P(IPAAm-DMAAm)-*b*-PLA micelles possessing OG units located the outermost surfaces. These results indicated that the effects of outermost surface functionalities such as OG and temperature-dependent diffusion changes across cellular membranes on intracellular uptake of micelles were negligible. The temperature-dependent internalization of thermoresponsive micelles was speculated to be attributed to the alternation of micellar characteristics including hydrophobicity and/or structural changes through the thermal phase transition of PID chains.

Flow cytometric study revealed that the intracellular uptake of thermoresponsive polymeric micelles was regulated by the temperature changes across the LCST. Cellular uptake depended on the incubation time, the micellar concentration, and the incubation temperature. P(IPAAm-DMAAm)-*b*-PLA micelles incubated at 42 °C were internalized with a relatively slow rate, compared with various nanoparticles (e.g., polystyrene beads), which are internalized inside cultured cells within 1 h.<sup>6,26</sup> Uptake rate of nanoparticles generally depends on intracellular uptake pathways and particle characteristics including morphology and size. Larger particles tend to be internalized inside the cell at a slow rate.<sup>6,27</sup> In our thermoresponsive micelle system, submicrometer-scale polymeric aggregates formed through intermicellar aggregations above the LCST. The size of polymeric aggregates seemed to affect the cellular uptake rate significantly. The ON/OFF intracellular uptake regulation was achieved by temperature cycles, which were related to the thermally induced hydrophilic/hydrophobic changes of the micellar coronas. In addition, we have previously investigated the effect of the polymeric architecture on thermally modulated intracellular uptake by comparing P(IPAAm-DMAAm)-*b*-PLA micelles with linear P(IPAAm-DMAAm).<sup>18</sup> Although intracellular uptake of linear P(IPAAm-DMAAm) was extremely low at temperatures both below and above the LCST, the thermoresponsive micelles showed intracellular uptake only above the LCST. A possible reason for tem-

perature-induced intracellular uptake is as follows. Below the LCST, corona-forming P(IPAAm-DMAAm) chains reduce the possible interactions of the PLA cores with cell surfaces. However, P(IPAAm-DMAAm) chains collapse and change to be a compact globule state through the dehydration of IPAAm units above the LCST, and then the interaction between hydrophobic PLA cores and the cell membranes is enhanced. As shown in Figure 4, the efficiency of micellar uptake was increased at higher incubation temperature, because the degree of dehydration and the compaction of thermoresponsive polymers became larger. As a result of promoted P(IPAAm-DMAAm) dehydration, the micellar aggregates enhanced the adhesion on cellular membranes and subsequent internalization inside cells.

**Analysis of Intracellular Uptake Mechanism.** For further understanding the intracellular micelle uptake system, the intracellular distributions and endocytosis pathways of micelles were investigated by confocal laser scanning microscopy (CLSM) and using endocytosis inhibitors for various pathways. In order to investigate which cellular organelles related to the micellar uptake, the intracellular distributions of the micelles were observed using various organelle-specific stain agents. Cell nuclei were selectively visualized (blue color) by Hoechst 33342 stain. The lysosomes (Figure 5A,B), and the Golgi apparatus and the endoplasmic reticulum (ER) (Figure 5C,D) were selectively stained in red. Yellow color means the coexistence of micelles and the respective stained cytoplasmic organelles. Below the LCST (37 °C), green fluorescents derived from OG-labeled polymeric micelles were scarcely detected in CLSM images (Figure 5A,C). On the contrary, the green colored dots of the micelles were clearly observed inside the cells around the cell nuclei above the LCST (42 °C) in the lysosome staining image (Figure 5B), indicating that the micelles were unable to localize inside the lysosomes. On the other hand, yellow colored dots were observed in the Golgi apparatus/ER staining image for the cells incubated with the micelles at 42 °C as shown in Figure 5D, and they maintained their colors more than 5 days. This result showed that the internalized micelles localized inside the Golgi apparatus/ER. Polymeric micelles are known to be transported to lysosomes via clathrin-mediated endocytosis.<sup>24,28</sup> The thermoresponsive micelles were transported to the Golgi apparatus/ER, meaning the relation with the caveolae-mediated endocytosis.<sup>29</sup> Moreover, since endothelial cells are abundant in caveolae domains on the cellular surface to generate caveolae-mediated endocytosis,<sup>30</sup> the intracellular uptake of

- (26) Rejman, J.; Oberle, V.; Zuhorn, I. S.; Hoekstra, D. Size-dependent internalization of particles via the pathways of clathrin- and caveolae-mediated endocytosis. *Biochem. J.* **2004**, *377* (1), 159–169.
- (27) Goldstein, J. L.; Anderson, R. G. W.; Brown, M. S. Coated pits, coated vesicles, and receptor-mediated endocytosis. *Nature* **1979**, *279*, 679–685.

- (28) Kakizawa, Y.; Kataoka, K. Block copolymer micelles for delivery of gene and related compounds. *Adv. Drug Delivery Rev.* **2002**, *54* (2), 203–222.
- (29) Sieczkarski, S. B.; Whittaker, G. R. Dissecting virus entry via endocytosis. *J. Gen. Virol.* **2002**, *83* (7), 1535–1545.
- (30) Schnitzer, J. E.; Oh, P.; Pinney, E.; Allard, J. Filipin-sensitive caveolae-mediated transport in endothelium: reduced transcytosis, scavenger endocytosis, and capillary permeability of select macromolecules. *J. Cell Biol.* **1994**, *127* (5), 1217–1232.

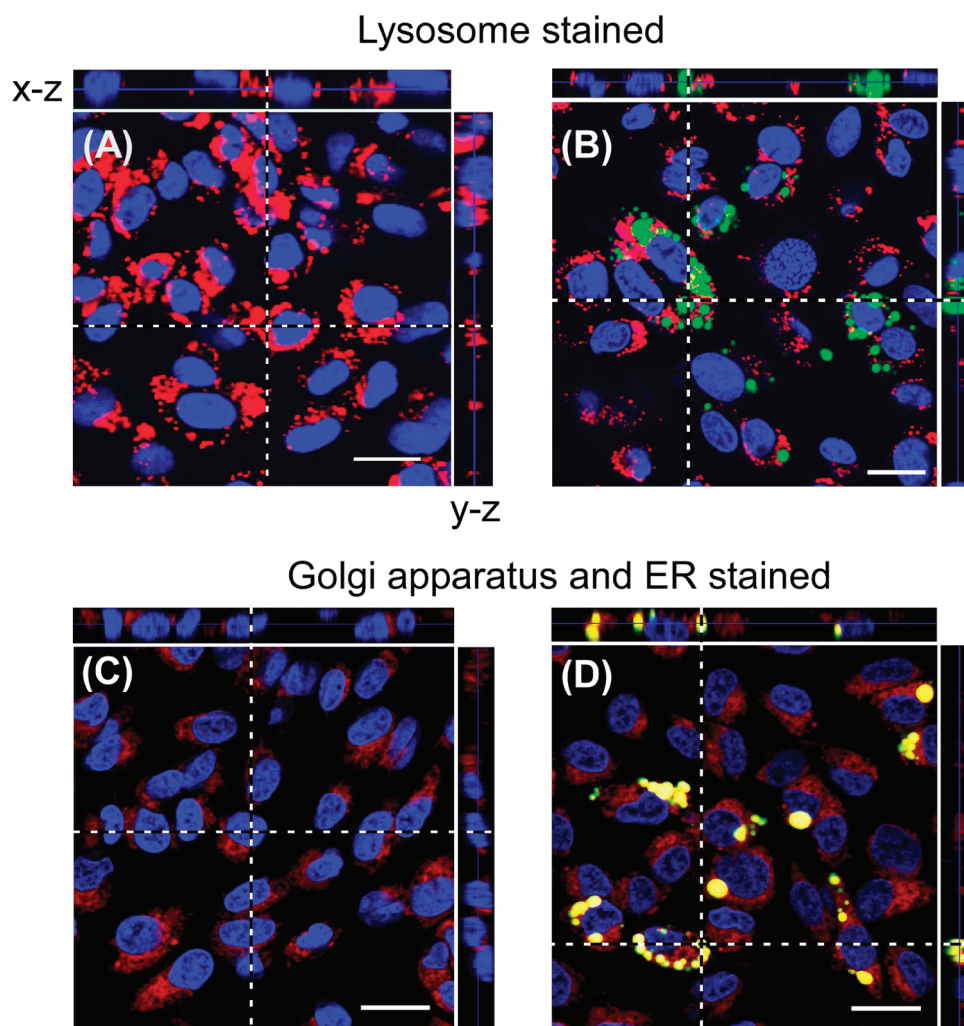


**Figure 5.** Triple fluorescent overlaid confocal laser scanning microscopic images of polymeric micelles localized within cultured cells after incubation for 6 h below the LCST (37 °C, A, C) and above the LCST (42 °C, B, D). The nuclei were stained with Hoechst 33258 (blue). Green fluorescence was derived from OG-labeled micelles. The following cellular organelles were selectively stained with red fluorescent reagents: lysosomes (A, B, with Lyso Tracker Red), and the Golgi apparatus and ER (C, D, with brefeldin A BODIPY 558/568 conjugate). Yellow colored dots indicated coexistence of the micelles and red stained organelles. Scale bars: 20  $\mu$ m.

thermoresponsive micelles in this study is possibly involved in the caveolae-mediated endocytosis.

Endocytosis pathways were further analyzed by incubation with the micelles in the presence of several endocytosis inhibitors above the LCST (42 °C) (Figure 6). Cytochalasin B<sup>31</sup> and amiloride<sup>32</sup> are known as micropinocytosis inhibitors, which mainly related to the intracellular uptake of more than submicrometer-scale macromolecules, and the efficiency of micelle uptake was reduced by 21 and 26% compared with that of the control cells. In our thermoresponsive micelle system, 600 nm aggregates were internalized inside the cells, and thus the intracellular uptake of thermoresponsive micelles was speculated to be possibly caused by micropinocytosis

mechanism. However, the internalization of particles by general micropinocytosis mechanism is known to go through lysosomes.<sup>29</sup> This matter conflicts with our observation that the cellular CLSM image shows nonlocalization in the lysosomes (Figure 4 B).

Clathrin-mediated endocytosis is commonly observed in macromolecule uptake mechanism<sup>28,33</sup> and is inhibited with chlorpromazine<sup>34</sup> and sucrose.<sup>35</sup> In our thermoresponsive system, chlorpromazine and sucrose decreased the efficiency

(31) Cooper, J. A. Effects of cytochalasin and phalloidin on actin. *J. Cell Biol.* **1987**, *105* (4), 1473–1478.

(32) West, M. A.; Bretscher, M. S.; Watts, C. Distinct endocytotic pathways in epidermal growth factor-stimulated human carcinoma A431 cells. *J. Cell Biol.* **1989**, *109* (6), 2731–2739.

(33) Kopecek, J.; Kopeckov, P.; Minko, T.; Lu, Z. R. HPMA copolymer-anticancer drug conjugates: design, activity, and mechanism of action. *Eur. J. Pharm. Biopharm.* **2000**, *50* (1), 61–81.

(34) Wang, L. H.; Rothberg, K. G.; Anderson, R. G. Mis-assembly of clathrin lattices on endosomes reveals a regulatory switch for coated pit formation. *J. Cell Biol.* **1993**, *123* (5), 1107–1117.

(35) Heuser, J. E.; Anderson, R. G. Hypertonic media inhibit receptor-mediated endocytosis by blocking clathrin-coated pit formation. *J. Cell Biol.* **1989**, *108* (2), 389–400.

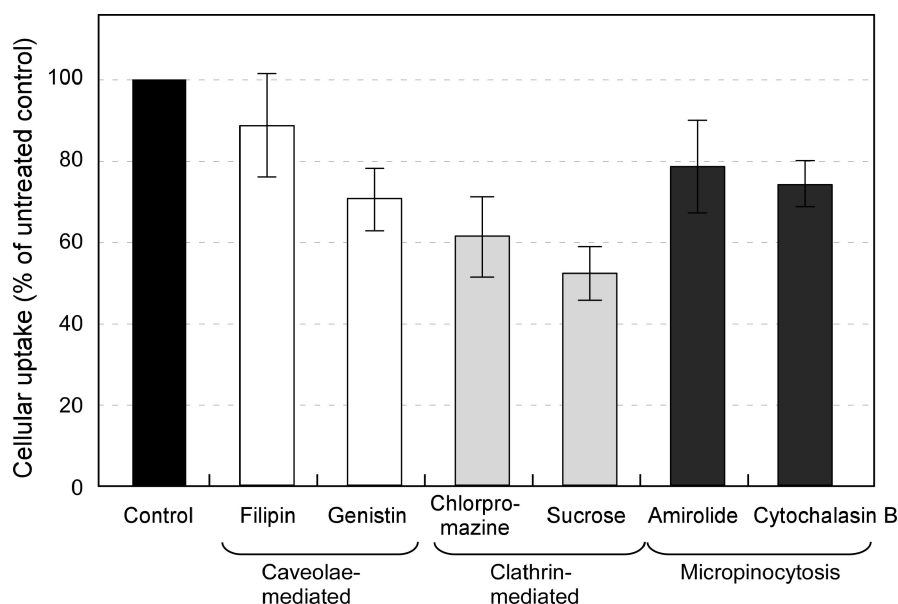


**Figure 6.** Effect of endocytosis inhibitors on the intracellular uptake of thermoresponsive polymeric micelles. Endothelial cells were preincubated with endocytosis inhibitors for 30 min at 37 °C, followed by incubation with thermoresponsive micelles at 42 °C for 3 h. Y axis: the mean of relative fluorescent intensity compared with the control cells. The circles and the bars show mean and SD, respectively ( $n = 4$ ).

of intracellular uptake by 39 and 52%, respectively, compared with the nontreated control cells with the inhibitors. For the route of clathrin-mediated endocytosis, particles are swallowed by cells in the form of clathrin-coated vesicles, which transport macromolecules to acidic lysosomes via early and late endosomes.<sup>29</sup> This route is employed for uptake of small nanoparticles (less than 150–200 nm) because of size limitation of clathrin-coated pits on cellular membrane.<sup>36</sup> Although endocytosis inhibiting test indicated the involvement of clathrin-mediated endocytosis and micropinocytosis, the thermoresponsive micelles were unable to be distributed in lysosomal compartments (Figure 4B). Decrease in cellular uptake by endocytosis inhibitors was probably due to the total decrease of cellular functions.

Furthermore, the possible cellular uptake of caveolae-mediated endocytosis was also investigated. In caveolae-mediated endocytosis pathway, macromolecules are transported to ER by caveosomes with bypassing lysosomes.<sup>29</sup> Caveolae-mediated endocytosis are inhibited with genistein<sup>37</sup> and filipin,<sup>30</sup> and reduced the cellular micelle uptake by 30 and 12%, respectively. Although caveolae-mediated endocytosis was unable to remarkably reduce by endocytosis inhibitors, the cellular CLSM image was consistent with the fact that the internalized particles via caveolae-mediated endocytosis were localized at the Golgi apparatus/ER (Figure 5D). However, the caveolae-mediated route is confined to nanoparticles with a diameter less than 60 nm<sup>36</sup> due to the size limitation of caveolae domains. In our thermoresponsive

micelle system, 600 nm aggregate, which was much larger than caveolae domains, employed intracellular uptake. Recently, the cellular uptake of submicrometer-scale nanoparticles was studied by nonphagocytic cells.<sup>6,26,38,39</sup> Rejman et al. report on the size-dependent variation of intracellular uptake pathways of anionic polystyrene beads and their intracellular localization.<sup>26</sup> Polystyrene beads with a diameter less than 200 nm are localized in the lysosomal compartments via clathrin-mediated endocytosis, while 500 nm beads are internalized inside the cells via caveolae-mediated endocytosis without localization in lysosomes. Other researchers also investigated the cellular uptake of cationic particles with a diameter more than 200 nm for mammal cells.<sup>6,26,38</sup> Especially, Gratton's group reported the intracellular uptake of large cationic nanoparticles (200–3000 nm), which are internalized inside the cells by various endocytosis mechanisms.<sup>6</sup> According to recent reports regarding endocytosis, intracellular uptake via clathrin- and caveolae-endocytosis is investigated by using particles with a diameter less than 200 nm. Our results suggested that a possible pathway for the P(IPAAm-DMAAm)-*b*-PLA micelles seemed to proceed through caveolae-mediated endocytosis route, regardless of the size of submicrometer-order particle. Although the uptake mechanism of thermoresponsive polymeric micelles is unclear in the present study, physicochemical properties (e.g., hydrophobicity, charge, size, and flexibility) of nanoparticles

(36) Conner, S. D.; Schmid, S. L. Regulated portals of entry into the cell. *Nature* **2003**, 422 (6927), 37–44.

(37) Chen, Y.; Norkin, L. C. Extracellular simian virus 40 transmits a signal that promotes virus enclosure within caveolae. *Exp. Cell Res.* **1999**, 246 (1), 83–90.

(38) Ogris, M.; Steinlein, P.; Kurs, M.; Mechtler, K.; Kirchheis, R.; Wagner, E. The size of DNA/transferrin-PEI complexes is an important factor for gene expression in cultured cells. *Gene Ther.* **1998**, 5 (10), 1425–1433.

(39) Rejman, J.; Bragonzi, A.; Conese, M. Role of clathrin- and caveolae-mediated endocytosis in gene transfer mediated by lipopolyplexes. *Mol. Ther.* **2005**, 12 (3), 468–474.

seem to play an important role to contribute to the intracellular micelle uptake.

Lysosome-bypassing endocytosis route may be preferable for the intracellular delivery of acid and/or enzyme-sensitive biomolecules such as nucleic acids or proteins. In general, the internalization of nanoscale particles inside cells was attributed by mainly clathrin-mediated pathway.<sup>28</sup> For the clathrin-mediated intracellular drug delivery of biomolecules including genes and proteins using nanoscale carriers, the endosomal escape of delivered biomolecules is one of the important factors to avoid their chemical decomposition by degradative enzymes and/or low pH (*ca.* 5.0) condition in lysosomal environment<sup>40</sup> and to express their pharmacological effects. Viruses are known to internalize inside cells via both clathrin- and caveolae-mediated pathways.<sup>41</sup> For example, gene delivery by virus-type vectors internalized genes through caveolae-mediated endocytosis with avoiding lysosomal decomposition and transport genes to ER by nonacidic caveosomes. The precise route for internalization of thermoresponsive micelles and transport mechanism to the Golgi apparatus/ER with acting as viruses was unclear. If particle sizes play an important role for internalization mechanism, intercellular delivery using submicrometer-scale particles (more than 500 nm) is significantly effective for biomolecule delivery *in vitro*.

Herein, this study successfully demonstrated to control the size and cellular interaction of thermoresponsive polymeric micelles by solely temperature changes. In our strategy using thermoresponsive micelles as a drug delivery tool, thermoresponsive polymeric micelles with drugs circulate in the bloodstream avoiding RES uptake and accumulate selectively at solid tumor tissues through EPR-mediated tumor targeting

below the micelle LCST. And then the thermoresponsive micellar corona chains change their properties and conformation by locally applied heating at the target sites upon the LCST. This alternation of micellar properties may promote selective drug actions and lysosome-bypassing intracellular uptake at only heated target site. Thermoresponsive polymeric micelle system is greatly attractive as delivery tools for bioactive molecules (e.g., gene and protein) as well as anticancer drugs.

## Conclusions

Temperature-induced intracellular uptake was investigated using fluorescent-labeled thermoresponsive polymeric micelles. The intracellular uptake of thermoresponsive micelles was successfully regulated by temperature modulation across the micellar LCST. Intracellular uptake above the micellar LCST was possibly caused by enhanced interactions between the micelles and cell membranes through the dehydration of thermoresponsive P(IPAAm-DMAAm) chains. The internalization of micelles was significantly affected by the micelle concentration, time, temperature, and cell viability. P(IPAAm-DMAAm)-*b*-PLA micelles localized at the Golgi apparatus/ER and were unable to be observed inside lysosome. These results indicate that thermoresponsive micelles are useful for convenient intracellular delivery of pH- and/or enzyme-sensitive drugs and biomolecules including nucleic acids, peptides, and proteins by the help of heating on target area.

**Acknowledgment.** The authors are grateful to Dr. N. Ueno (Tokyo Women's Medical University) for his valuable comments and manuscript editing. This work was financially supported by NEDO Special Courses for Development of Innovative Drug Delivery Systems funded by New Energy and Industrial Technology Development Organization (NEDO), Japan, and Global COE program "Center for Practical Chemical Wisdom" supported by Ministry of Education, Culture, Sports, Science and Technology (MEXT).

MP100021C

(40) Murphy, R. F.; Powers, S.; Cantor, C. R. Endosome pH measured in single cells by dual fluorescence flow cytometry: rapid acidification of insulin to pH 6. *J. Cell Biol.* **1984**, *98* (5), 1757–1762.

(41) Le, P. U.; Nabi, I. R. Distinct caveolae-mediated endocytic pathways target the Golgi apparatus and the endoplasmic reticulum. *J. Cell Sci.* **2003**, *116* (6), 1059–1071.